

X-921-77-9

PREPRINT

NASA TM X-71265

SEISMIC EFFECTS ON THE ROTATIONAL DYNAMICS OF THE EARTH AND ITS GRAVITATIONAL FIELD

(NASA-TM-X-71265) SEISMIC EFFECTS ON THE ROTATIONAL DYNAMICS OF THE EARTH AND ITS GRAVITATIONAL FIELD (NASA) 53 P
HC A04/MF A01

N77-16484

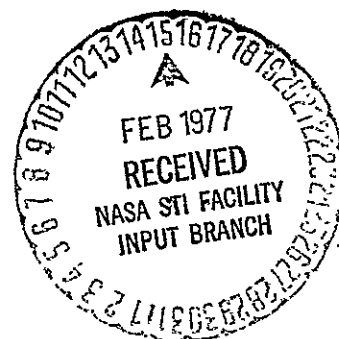
CSCI 08K

G3/46

Unclas
13825

BRAULIO V. SANCHEZ

DECEMBER 1976



— GODDARD SPACE FLIGHT CENTER —
GREENBELT, MARYLAND

**For information concerning availability
of this document contact:**

**Technical Information Division, Code 250.
Goddard Space Flight Center
Greenbelt, Maryland 20771**

(Telephone 301-982-4488)

**"This paper presents the views of the author(s), and does not necessarily
reflect the views of the Goddard Space Flight Center, or NASA."**

SEISMIC EFFECTS ON THE ROTATIONAL DYNAMICS OF
THE EARTH AND ITS GRAVITATIONAL FIELD

Braulio V. Sanchez

December 1976

GODDARD SPACE FLIGHT CENTER
Greenbelt, Maryland

SEISMIC EFFECTS ON THE ROTATIONAL DYNAMICS OF
THE EARTH AND ITS GRAVITATIONAL FIELD

Braulio V. Sanchez

December 1976

GODDARD SPACE FLIGHT CENTER
Greenbelt, Maryland

ACKNOWLEDGMENTS

I express my appreciation to the National Research Council, the National Academy of Sciences and the Goddard Space Flight Center for providing the necessary support. In particular I convey my thanks to Dr. David Smith of the Geodynamics Branch.

This investigation would not have been possible without the cooperation of Mr. George H. Wyatt who provided advise and support with the numerical analysis aspects of the problem.

I also give thanks to Mrs. Barbara Putney for her professional help and to Mrs. Beatrice Boccucci for her secretarial support.

Finally, I give thanks to all those who have helped in the process of completing this project.

CONTENTS

	<u>Page</u>
ACKNOWLEDGMENTS	iii
INTRODUCTION	1
1. RELATION BETWEEN MOMENT OF INERTIA, ROTATION AND FAULTING	2
2. RECIPROCAL THEOREM AND VOLTERRA'S FORMULA	3
3. RELATION BETWEEN MOMENT OF INERTIA AND VOLTERRA'S FORMULA	5
4. MOMENTS AND PRODUCTS OF INERTIA	6
5. STRESSES	8
6. RADIAL FUNCTIONS	10
7. THE ROTATIONAL POTENTIAL	14
8. SOURCE PARAMETERS	16
9. OUTLINE OF PROCEDURE	18
10. NUMERICAL PROCEDURE	19
11. NUMERICAL RESULTS AND CONCLUSIONS	35
REFERENCES	39

ILLUSTRATIONS

<u>Figure</u>	<u>Page</u>
8.1 Source Parameters	17
10.1 y_1 vs. r , Model P	23

PRECEDING PAGE BLANK NOT FILMED

ILLUSTRATIONS (Continued)

<u>Figure</u>	<u>Page</u>
10.2 y_2 , vs. r , Model P	24
10.3 y_3 vs. r , Model P	25
10.4 y_4 vs. r , Model P	26
10.5 y_5 vs. r , Model P	27
10.6 y_6 vs. r , Model P	28
10.7 y_1 vs. r , Model M_3	29
10.8 y_2 vs. r , Model M_3	30
10.9 y_3 vs. r , Model M_3	31
10.10 y_4 vs. r , Model M_3	32
10.11 y_5 vs. r , Model M_3	33
10.12 y_6 vs. r , Model M_3	34

TABLES

<u>Table</u>	<u>Page</u>
11.1 Pole Shift (cm).	42
11.2 Angle (Degrees)	42
11.3 $\Delta\text{LOD}(\text{sec}) \times 10^8$	43
11.4 $\Delta C_{20} \times 10^{10}$	43
11.5 $\Delta C_{21} \times 10^{10}$	44
11.6 $\Delta S_{21} \times 10^{10}$	44

TABLES (Continued)

<u>Table</u>		<u>Page</u>
11.7	$\Delta C_{22} \times 10^{11}$	45
11.8	$\Delta S_{22} \times 10^{11}$	45

INTRODUCTION

A study of the effects of earthquakes on the rotational motion of the earth has been conducted. The analytical developments providing the connection between the fault parameters and the corresponding changes in the moments and products of inertia are due to Rice and Chinnery (1972), the method involves the application of the reciprocal theorem of elasticity and Volterra's formula as well as the displacement and stress fields for the second degree static response of the earth model being used.

Two earth models have been used in the investigation, the parametric model due to Dziewonski, Hales and Lapwood (1975) and the M_3 model of Landisman, Sato and Nafe (1965) as given by Israel, Ben-Menahem and Singh (1973).

In order to obtain the displacement and stress fields it is necessary to integrate numerically a system of differential equations representing the state of equilibrium of an elastic body. The numerical integration problem presents certain aspects which require consideration; some of these aspects are the following: the conditions in a neighborhood close to the origin, at which the differential equations become singular; and the appropriate boundary conditions between the solid and the liquid parts of the body.

The numerical results of the investigation yield the magnitude and direction of the pole shift as well as the change in the length of the day. In addition, the changes in the second degree coefficients of the geopotential have been computed.

In order to generate numerical results the source parameters corresponding to the Alaskan earthquake on March 28, 1964 were chosen, as given by Israel et al., 1973.

1. RELATION BETWEEN MOMENT OF INERTIA, ROTATION AND FAULTING

Consider a body of mass M rotating with angular velocity $\vec{\omega}$ and let the axis L be defined by the direction of $\vec{\omega}$.

The moment of inertia with respect to the axis L is defined by

$$I_L = \int_M d_0^2 dm \quad (1.1)$$

d_0 is the perpendicular distance from the element of mass dm to the axis L . Assume a displacement field to be defined throughout the body due to causes other than rotation, i. e., as a result of faulting. The perpendicular distance from dm to the axis L is now given by

$$d = d_0 + \Delta d \quad (1.2)$$

where Δd denotes the component of displacement due to faulting perpendicular to L . The moment of inertia is now given by

$$I_L = \int_M d^2 dm \quad (1.3)$$

substituting Equation (1.2) into Equation (1.3) yields,

$$I_L = \int_M d_0^2 dm + 2 \int_M (d_0 \Delta d) dm + \int_M \Delta d^2 dm \quad (1.4)$$

Assume Δd to be small enough so that the term containing Δd^2 can be neglected, then

$$\Delta I_L = 2 \int_M (d_0 \Delta d) dm \quad (1.5)$$

where ΔI_L stands for the increment in the moment of inertia due to faulting.

Now, the rotational potential is given by

$$T = \frac{1}{2} \omega^2 d_0^2 \quad (1.6)$$

and the corresponding force by

$$\frac{\partial T}{\partial d_0} = \omega^2 d_0 \quad (1.7)$$

Therefore,

$$d_0 = \frac{1}{\omega^2} \frac{\partial T}{\partial d_0} \quad (1.8)$$

substituting Equation (1.8) into Equation (1.5) yields

$$\Delta I_L = \frac{2}{\omega^2} \int_M \left(\frac{\partial T}{\partial d_0} \Delta d \right) dm \quad (1.9)$$

2. RECIPROCAL THEOREM AND VOLTERRA'S FORMULA

The Reciprocal Theorem of elasticity is due to E. Betti, its proof can be found in the book by Love (1944), more recently Smylie and Mansinha (1971) and Rice and Chinnery (1972) have extended it to the case of self-gravitating elastic systems in states of large initial hydrostatic stress. The presentation which follows is due to Rice and Chinnery (1972).

Consider a body of mass M and a surface Σ within the body, define the following:

\hat{n}^+, \hat{n}^- : unit vectors normal to an element of surface $d\Sigma$, opposite in direction, with \hat{n}^- pointing from $d\Sigma^-$ to $d\Sigma^+$.

\vec{u} : a displacement field defined throughout M with a discontinuity, $\Delta\vec{u} = \vec{u}^+ - \vec{u}^-$, due to slip, defined on Σ ,

$[\sigma]$: stress field defined throughout M , due to \vec{u} .

\vec{f}^* : a body force field, defined throughout M , independent of \vec{u} .

\vec{u}^* : a displacement field defined throughout M , due to the application of \vec{f}^* .

$[\sigma^*]$: stress field defined throughout M , due to \vec{u}^* .

Assume the following conditions to hold:

- i. $[\sigma]$ and $[\sigma^*]$ vanish at the outer surface of the body.
- ii. $[\sigma^*]$ and \vec{u}^* are continuous across Σ since they are produced by \vec{f}^* , with no slip on Σ .
- iii. $(\hat{n} \cdot [\sigma])^+ + (\hat{n} \cdot [\sigma])^- = 0$, this last condition implies equilibrium after slip.

The Reciprocal Theorem states that the work done by the body force \vec{f}^* and the stress $[\sigma^*]$ acting through the displacements \vec{u} is equal to the work done by the stresses $[\sigma]$ acting through the displacements \vec{u}^* . Therefore,

$$\begin{aligned} \int_M (\vec{f}^* \cdot \vec{u}) dm + \int_\Sigma \left\{ (\hat{n} \cdot [\sigma^*] \cdot \vec{u})^+ + (\hat{n} \cdot [\sigma^*] \cdot \vec{u})^- \right\} d\Sigma \\ = \int_\Sigma \left\{ (\hat{n} \cdot [\sigma] \cdot \vec{u}^*)^+ + (\hat{n} \cdot [\sigma] \cdot \vec{u}^*)^- \right\} d\Sigma \end{aligned} \quad (2.1)$$

By virtue of conditions (ii.) and (iii.) Equation (2.1) can be written as:

$$\int_M (\vec{f}^* \cdot \vec{u}) dm = \int_\Sigma (\hat{n} \cdot [\sigma^*] \cdot \Delta \vec{u}) d\Sigma \quad (2.2)$$

with $\hat{n} = \hat{n}^-$, now let $\Delta \vec{u} = (\Delta u) \hat{s}$, \hat{s} being a unit vector in the direction of slip.

Furthermore define

$$\tau^* = \hat{n} \cdot [\sigma^*] \cdot \hat{s} \quad (2.3)$$

Equation (2.2) can then be written as

$$\int_M (\vec{f}^* \cdot \vec{u}) dm = \int_\Sigma \tau^* (\Delta u) d\Sigma \quad (2.4)$$

Equation (2.4) is referred to as Volterra's formula.

3. RELATION BETWEEN MOMENT OF INERTIA AND VOLTERRA'S FORMULA

Consider the integrand in the left side of Equation (2.4), let \vec{f}^* denote a body force due to rotation as given by Equation (1.7) and let \vec{u} stand for the displacement field due to faulting, Equations (1.9) and (2.4) then yield

$$\Delta I_L = \frac{2}{\omega^2} \int_{\Sigma} \tau_L^* (\Delta u) d\Sigma \quad (3.1)$$

where

$$\tau_L^* = \hat{n} \cdot [\sigma^*]_L \cdot \hat{s} \quad (3.2)$$

$[\sigma^*]_L$ being the stresses due to the rotation about the axis L. The stress tensor $[\sigma^*]_L$ contains a factor ω^2 which will cancel the same factor appearing in the denominator on the right side of Equation (3.1), this will be shown below.

4. MOMENTS AND PRODUCTS OF INERTIA

Consider the inertia dyadic,

$$[I] = \begin{bmatrix} I_{xx} \hat{i} \hat{i} & -I_{xy} \hat{i} \hat{j} & -I_{xz} \hat{i} \hat{k} \\ -I_{xy} \hat{j} \hat{i} & I_{yy} \hat{j} \hat{j} & -I_{yz} \hat{j} \hat{k} \\ -I_{xz} \hat{k} \hat{i} & -I_{yz} \hat{k} \hat{j} & I_{zz} \hat{k} \hat{k} \end{bmatrix} \quad (4.1)$$

Note that,

$$\begin{aligned} \hat{i} \cdot [I] \cdot \hat{i} &= I_{xx} \\ \hat{j} \cdot [I] \cdot \hat{j} &= I_{yy} \\ \hat{k} \cdot [I] \cdot \hat{k} &= I_{zz} \end{aligned} \quad (4.2)$$

Define the following unit vectors:

$$\begin{aligned} \hat{r} &= (1/\sqrt{2})(\hat{i} + \hat{j}) \\ \hat{m} &= (1/\sqrt{2})(\hat{i} - \hat{j}) \\ \hat{q} &= (1/\sqrt{2})(\hat{k} + \hat{j}) \\ \hat{p} &= (1/\sqrt{2})(\hat{k} - \hat{j}) \\ \hat{o} &= (1/\sqrt{2})(\hat{k} - \hat{i}) \end{aligned} \quad (4.3)$$

$$\hat{q} = (1/\sqrt{2})(\hat{k} + \hat{i}) \quad (4.3)$$

(cont.)

Then,

$$\begin{aligned} \hat{m} \cdot [I] \cdot \hat{m} - \hat{r} \cdot [I] \cdot \hat{r} &= 2I_{xy} \\ \hat{p} \cdot [I] \cdot \hat{p} - \hat{l} \cdot [I] \cdot \hat{l} &= 2I_{yz} \\ \hat{o} \cdot [I] \cdot \hat{o} - \hat{q} \cdot [I] \cdot \hat{q} &= 2I_{xz} \end{aligned} \quad (4.4)$$

Equations (3.1), (4.2) and (4.4) then yield

$$\begin{aligned} \Delta I_{xx} &= \frac{2}{\omega^2} \int_{\Sigma} \tau_x^*(\Delta u) d\Sigma \\ \Delta I_{yy} &= \frac{2}{\omega^2} \int_{\Sigma} \tau_y^*(\Delta u) d\Sigma \\ \Delta I_{zz} &= \frac{2}{\omega^2} \int_{\Sigma} \tau_z^*(\Delta u) d\Sigma \\ \Delta I_{xy} &= \frac{1}{\omega^2} \int_{\Sigma} \tau_m^*(\Delta u) d\Sigma - \frac{1}{\omega^2} \int_{\Sigma} \tau_r^*(\Delta u) d\Sigma \\ \Delta I_{yz} &= \frac{1}{\omega^2} \int_{\Sigma} \tau_p^*(\Delta u) d\Sigma - \frac{1}{\omega^2} \int_{\Sigma} \tau_l^*(\Delta u) d\Sigma \\ \Delta I_{xz} &= \frac{1}{\omega^2} \int_{\Sigma} \tau_o^*(\Delta u) d\Sigma - \frac{1}{\omega^2} \int_{\Sigma} \tau_q^*(\Delta u) d\Sigma \end{aligned} \quad (4.5)$$

As indicated by Equation (3.2) the quantities τ_x^* , τ_y^* , ..., τ_q^* denote the shear stresses induced on Σ by rotation about the axis indicated by the subscript.

If the seismic event is assumed to be represented by a point source then Equations (4.5) can be written as follows.

$$\begin{aligned}
\Delta I_{xx} &= 2K\tau_x^* \\
\Delta I_{yy} &= 2K\tau_y^* \\
\Delta I_{zz} &= 2K\tau_z^* \\
\Delta I_{xy} &= K(\tau_m^* - \tau_r^*) \\
\Delta I_{yz} &= K(\tau_p^* - \tau_l^*) \\
\Delta I_{xz} &= K(\tau_o^* - \tau_q^*)
\end{aligned} \tag{4.6}$$

where

$$K = (1/\omega^2)(\Delta u)(\Sigma) \tag{4.7}$$

5. STRESSES

Equations (4.5) and (3.2) require knowledge of the stresses produced on Σ by rotation about a certain axis, this constitutes a part of a more general problem which is briefly outlined below.

The equations of motion governing the vibrations of an elastic body are given by Love (1944):

$$(\lambda + \mu) \left(\frac{\partial \Delta}{\partial x}, \frac{\partial \Delta}{\partial y}, \frac{\partial \Delta}{\partial z} \right) + \mu \nabla^2 \mathbf{U} + \rho \nabla V = \rho \frac{\partial^2}{\partial t^2} \mathbf{U} \tag{5.1}$$

$$\Delta = \frac{\partial u_x}{\partial x} + \frac{\partial u_y}{\partial y} + \frac{\partial u_z}{\partial z} \tag{5.2}$$

$$\mathbf{U} = (u_x, u_y, u_z) \tag{5.3}$$

The body force potential V is given by

$$V = V_0 + \psi \tag{5.4}$$

where ψ denotes the perturbation from the undisturbed state V_0 . V must obey Poisson's equation:

$$\nabla^2 V = -4\pi G\rho \quad (5.5)$$

Let the disturbing potential be given

$$T_n = (r/a)^n S_n(\theta, \phi) \quad (5.6)$$

where S_n denotes a surface spherical harmonic and a the radius of the earth.

Equations (5.1) and (5.5) can be expressed in spherical coordinates and with the appropriate set of boundary conditions they will admit the following eigen vector solutions:

$$\begin{aligned} u_r &= y_1(r)S_n \\ u_\theta &= y_3(r) \frac{\partial S_n}{\partial \theta} \\ u_\phi &= \frac{y_3(r)}{\sin \theta} \frac{\partial S_n}{\partial \phi} \end{aligned} \quad (5.7)$$

The stress-strain relations yield:

$$\begin{aligned} \sigma_{rr} &= y_2(r)S_n \\ \sigma_{r\theta} &= y_4(r) \frac{\partial S_n}{\partial \theta} \\ \sigma_{r\phi} &= \frac{y_4(r)}{\sin \theta} \frac{\partial S_n}{\partial \phi} \\ \sigma_{\theta\theta} &= \left[\frac{2}{r} (\lambda + \mu)y_1 + \lambda \dot{y}_1 - \frac{n(n+1)}{r} \lambda y_3 \right] S_n + \left(\frac{2\mu}{r} y_3 \right) \frac{\partial^2 S_n}{\partial \theta^2} \end{aligned} \quad (5.8)$$

$$\begin{aligned} \sigma_{\phi\phi} = & \left[\frac{2}{r} (\lambda + \mu) \dot{y}_1 + \lambda \dot{y}_1 - \frac{n(n+1)}{r} \lambda y_3 \right] S_n \\ & + \left(\frac{2\mu}{r} \cot \theta y_3 \right) \frac{\partial S_n}{\partial \theta} + \left(\frac{2\mu}{r \sin^2 \theta} y_3 \right) \frac{\partial^2 S_n}{\partial \phi^2} \\ & \sigma_{\theta\phi} = \left(-\frac{2\mu}{r} \frac{\cot \theta}{\sin \theta} y_3 \right) \frac{\partial S_n}{\partial \phi} + \left(\frac{\mu}{r \sin^2 \theta} y_3 \right) \frac{\partial^2 S_n}{\partial \phi^2} \\ & + \left(\frac{\mu}{r \sin \theta} y_3 \right) \frac{\partial^2 S_n}{\partial \phi \partial \theta} \end{aligned} \quad \begin{array}{l} (5.8) \\ \text{(cont.)} \end{array}$$

where,

$$\begin{aligned} y_2 &= \lambda \left[\dot{y}_1 + \frac{2}{r} y_1 - \frac{n(n+1)}{r} y_3 \right] + 2\mu \dot{y}_1 \\ y_4 &= \mu \left(\dot{y}_3 - \frac{y_3}{r} + \frac{y_1}{r} \right) \end{aligned} \quad (5.9)$$

The time-dependent solution $e^{if_n t}$ has been omitted from Equations (5.7) and (5.8). The dots denote (d/dr) . The stresses given by Equation (5.8) are those produced by the action of the disturbing potential T_n and do not include the initial hydrostatic stress.

6. RADIAL FUNCTIONS

The radial functions y_1 , y_2 , y_3 and y_4 appearing in Equations (5.7) and (5.8) have to be obtained by numerical integration when working with models resembling the real Earth. In addition define

$$\psi = y_5(r) S_n(\theta, \phi) \quad (6.1)$$

$$y_6 = \dot{y}_5 - 4\pi G \rho_0 y_1 \quad (6.2)$$

Equations (5.1) and (5.5) can then be expressed as a system of six ordinary differential equations (Alterman et al., 1959)

$$\dot{\vec{y}} = [M]\vec{y} \quad (6.3)$$

$$\vec{y} = (y_1, y_2, y_3, y_4, y_5, y_6)^T \quad (6.4)$$

The static or steady-state solution is obtained by letting the frequency f_n be equal to zero. The elements of the matrix M are given by Smylie and Mansinha (1971) and Israel et al. (1973). They are given below for the sake of completeness. The symbols ρ_0 , μ and λ denote the density and the elastic parameters, g_0 stands for the gravitational acceleration and n is the degree of the deformation, in this case $n = 2$.

Let

$$\begin{aligned} c &= 1/(\lambda + 2\mu) \\ M_{11} &= -2\lambda c/r \\ M_{12} &= c \\ M_{13} &= n(n+1)c/r \\ M_{21} &= 4\mu(3\lambda + 2\mu)c/r^2 - 4\rho_0 g_0/r \\ M_{22} &= -4\mu c/r \\ M_{23} &= -n(n+1)[2\mu(3\lambda + 2\mu)c/r^2 - \rho_0 g_0/r] \\ M_{24} &= n(n+1)/r \\ M_{26} &= -\rho_0 \\ M_{31} &= -1/r \\ M_{33} &= 1/r \end{aligned} \quad (6.5)$$

$$\begin{aligned}
M_{34} &= 1/\mu \\
M_{41} &= -2\mu(3\lambda + 2\mu)c/r^2 + \rho_0 g_0/r \\
M_{42} &= -\lambda c/r \\
M_{43} &= 4n(n+1)\mu(\lambda + \mu)c/r^2 - 2\mu/r^2 \\
M_{44} &= -3/r \\
M_{45} &= -\rho_0/r \\
M_{51} &= 4\pi G\rho_0 \\
M_{56} &= 1 \\
M_{63} &= -4\pi Gn(n+1)\rho_0/r \\
M_{65} &= n(n+1)/r^2 \\
M_{66} &= -2/r
\end{aligned}
\tag{6.5}$$

(cont.)

all the other elements are equal to zero.

Equations (6.3) and (6.5) are applicable to the solid regions of the earth.

The equations for the liquid core have been developed by Smylie and Mansinha (1971) and Israel et al. (1973), they are given below:

$$\begin{aligned}
y_1 &= y_5/g_0 \\
y_2 &= 0 \\
y_3 &= (4y_5 + ry_6)/n(n+1)g_0 \\
y_4 &= 0 \\
\dot{y}_5 &= (4\pi G\rho_0 y_5)/g_0 + y_6 \\
\dot{y}_6 &= [n(n+1)/r^2 - 16\pi G\rho_0/g_0 r]y_5 - (4\pi G\rho_0/g_0 + 2/r)y_6
\end{aligned}
\tag{6.6}$$

The following assumptions are implicit in the set of Equation (6.6):

- i. the liquid core is in a state of hydrostatic equilibrium before and after the deformation, this means that the tangential stresses are equal to zero.
- ii. the dilatation and the normal stress are equal to zero. Zero dilatation is consistent with constant core volume and makes the Adams-Williamson condition unnecessary.

Equations (6.3) and (6.6) have to satisfy certain conditions at the boundaries between the solid and the liquid parts of the earth, there has been some debate in the literature concerning this issue. The conditions given below are those developed by Israel et al. (1973) and Crossley and Gubbins (1975), at least with respect to the condition for the variable y_6 . Let $\{y_i\}$ denote the jump (discontinuity) in the variable y_i at the boundary between the liquid and the solid parts, then

$$\begin{aligned}
 \{y_1\} &= \text{some constant} \\
 \{y_2\} &= \rho_0 g_0 \{y_1\} \\
 \{y_3\} &= \text{some constant} \\
 \{y_4\} &= 0 \\
 \{y_5\} &= 0 \\
 \{y_6\} &= -4\pi G \rho_0 \{y_1\}
 \end{aligned}
 \tag{6.7}$$

Note that Equations (6.7) imply the continuity of y_4 and y_5 .

Alterman et al. (1959) developed the remaining boundary conditions to be imposed on the differential equations. At the deformed surface of the earth the stresses must vanish and the gravitational potential and its gradient must be continuous, i. e.,

$$\begin{aligned} y_2(a) &= 0 \\ y_4(a) &= 0 \\ y_6(a) + \frac{(n+1)}{a} y_5(a) &= b \end{aligned} \quad (6.8)$$

where a denotes the radius of the earth and b is a constant with a value depending on the nature of the disturbance as shown by Takeuchi et al. (1962). In particular, for the earth-tide problem:

$$b = (2n+1)/a \quad (6.9)$$

Implicit in Equation (6.9) is the assumption that the disturbing potential is given by Equation (5.6).

7. THE ROTATIONAL POTENTIAL

The rotational potential as given by Equation (1.6) can be expressed in the form of Equation (5.6) (Sanchez, 1974):

$$T_2 = (r/a)^2 S_2(\theta, \phi) \quad (7.1)$$

where

$$S_2(\theta, \phi) = \sum_{m=0}^2 P_2^m(\cos \theta) (a_2^m \cos m\phi + u_2^m \sin m\phi) \quad (7.2)$$

$$\begin{aligned}
q_2^0 &= (a^2/6)(\omega_x^2 + \omega_y^2 - 2\omega_z^2) \\
q_2^1 &= -(a^2/3)(\omega_x \omega_z) \\
u_2^1 &= -(a^2/3)(\omega_y \omega_z) \\
q_2^2 &= (a^2/12)(\omega_y^2 - \omega_x^2) \\
u_2^2 &= -(a^2/6)(\omega_x \omega_y)
\end{aligned} \tag{7.3}$$

Equation (7.1) does not include a term equal to $(1/3)(\omega_x^2 + \omega_y^2 + \omega_z^2)$ which produces expansion or contraction of the body as a whole, such a deformation will affect the moments of inertia.

The stress tensor which appears in Equations (3.2) and (4.5) requires the evaluation of the stresses given by Equation (5.8), the stresses are produced by rotation about a certain axis, the components of rotation ω_x , ω_y and ω_z appearing in Equations (7.3) will take values corresponding to the axis:

$$\begin{aligned}
(\omega_x, \omega_y, \omega_z)_x &= (\omega, 0, 0) \\
(\omega_x, \omega_y, \omega_z)_y &= (0, \omega, 0) \\
(\omega_x, \omega_y, \omega_z)_z &= (0, 0, \omega) \\
(\omega_x, \omega_y, \omega_z)_r &= (1/\sqrt{2})(\omega, \omega, 0) \\
(\omega_x, \omega_y, \omega_z)_m &= (1/\sqrt{2})(\omega, -\omega, 0) \\
(\omega_x, \omega_y, \omega_z)_l &= (1/\sqrt{2})(0, \omega, \omega) \\
(\omega_x, \omega_y, \omega_z)_p &= (1/\sqrt{2})(0, -\omega, \omega) \\
(\omega_x, \omega_y, \omega_z)_o &= (1/\sqrt{2})(-\omega, 0, \omega) \\
(\omega_x, \omega_y, \omega_z)_q &= (1/\sqrt{2})(\omega, 0, \omega)
\end{aligned} \tag{7.4}$$

8. SOURCE PARAMETERS

The shear stresses given by Equation (3.2) contain the source parameters \hat{n} and \hat{s} as well as the stress tensor due to rotation. The stresses given by Equations (5.8) are computed in a spherical system of coordinates, the source parameters \hat{n} and \hat{s} are usually given in an epicentral coordinate system, the necessary transformations are given below:

$$\begin{aligned} \tau^* = & n_r \sigma_{rr} s_r + n_\theta \sigma_{\theta\theta} s_\theta + n_\phi \sigma_{\phi\phi} s_\phi + 2(n_r \sigma_{r\theta} s_\theta + n_\theta \sigma_{r\theta} s_r) \\ & + 2(n_r \sigma_{r\phi} s_\phi + n_\phi \sigma_{r\phi} s_r) + 2(n_\theta \sigma_{\theta\phi} s_\phi + n_\phi \sigma_{\theta\phi} s_\theta) \end{aligned} \quad (8.1)$$

The following transformations are given by Israel et al. (1973), Figure 8.1 below is taken from that work:

$$\begin{Bmatrix} \hat{s} \\ \hat{n} \end{Bmatrix} = \begin{Bmatrix} \cos \lambda & \sin \lambda \cos \delta & \sin \lambda \sin \delta \\ 0 & -\sin \delta & \cos \delta \end{Bmatrix} \begin{Bmatrix} \hat{e}_1 \\ \hat{e}_2 \\ \hat{e}_3 \end{Bmatrix} \quad (8.2)$$

$$\begin{Bmatrix} \hat{e}_1 \\ \hat{e}_2 \\ \hat{e}_3 \end{Bmatrix} = \begin{Bmatrix} -\cos \alpha & \sin \alpha & 0 \\ -\sin \alpha & -\cos \alpha & 0 \\ 0 & 0 & 1 \end{Bmatrix} \begin{Bmatrix} \hat{e}_\theta \\ \hat{e}_\phi \\ \hat{e}_r \end{Bmatrix} \quad (8.3)$$

Making use of Equations (8.2) and (8.3) yields:

$$\begin{aligned} s_r &= \sin \lambda \sin \delta \\ s_\theta &= -\cos \lambda \cos \alpha - \sin \lambda \cos \delta \sin \alpha \\ s_\phi &= \cos \lambda \sin \alpha - \sin \lambda \cos \delta \cos \alpha \\ n_r &= \cos \delta \\ n_\theta &= \sin \delta \sin \alpha \\ n_\phi &= \sin \delta \cos \alpha \end{aligned} \quad (8.4)$$

where

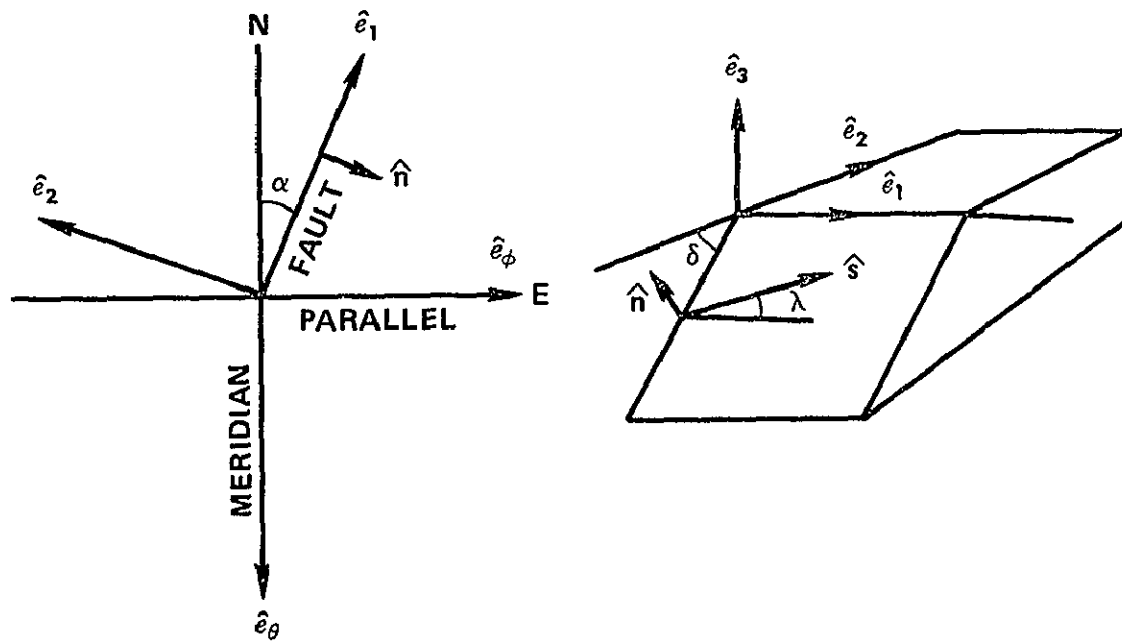


Figure 8.1. Source Parameters

- δ : dip angle
 λ : slip angle
 α : azimuth angle

9. OUTLINE OF PROCEDURE

The numerical results which are given in the last section were obtained by assuming the seismic event to be represented by a point source. The following is an outline of the procedure.

- A. Given h (source depth) integrate the system of differential equations given by Equations (6.3) - (6.6) to obtain $(y_1, y_2, y_3, \dot{y}_1)$ at the corresponding value of r .
- B. Choose an axis of rotation, the corresponding set $(\omega_x, \omega_y, \omega_z)$ will be given by Equations (7.4), ω can be set equal to 1.
- C. Using the results of step B and Equation (7.3) compute $q_2^0, q_2^1, u_2^1, q_2^2, u_2^2$ for each axis of rotation.
- D. Given θ and ϕ (colatitude and longitude of the source) compute S_2 and its derivatives for each rotation axis by means of Equation (7.2) and the results of step C.
- E. Using the results of steps A and D and Equations (5.8) compute $\sigma_{rr}, \sigma_{r\theta}, \sigma_{r\phi}, \sigma_{\theta\theta}, \sigma_{\phi\phi}, \sigma_{\theta\phi}$ for each rotation axis.

- F. Given δ , λ , α (dip, slip and azimuth of the fault) compute s_r , s_θ , s_ϕ , n_r , n_θ , n_ϕ as given by Equations (8.4).
- G. Using the results of steps E and F and Equation (8.1) compute τ^* for each rotation axis.
- H. Given Δu , Σ (slip magnitude and fault area) and using the results of step G compute the changes in the moments and products of inertia by means of Equations (4.6).
- I. Use the results of step H to compute the magnitude and direction of the pole shift as well as the change in the length of the day. It is possible also to compute the changes in the second degree coefficients of the geopotential.

10. NUMERICAL PROCEDURE

The numerical integration of the system of differential equations given by Equation (6.3) - (6.6) requires the adoption of an earth model giving the radial distribution of density ρ and the elastic parameters μ and λ . The two earth models used in this investigation are the following:

- i. the parametric earth model due to Dziewonski, Hales and Lapwood (1975) in which radial variations of density and elastic parameters are represented by piecewise continuous analytical functions of the radius.

In particular the model representing a continental structure was used and it is referred to as the P model below.

- ii. the model M_3 of Landisman, Sato and Nafe (1965) as given by Israel, Ben-Menahem and Singh (1973). The density and elastic parameters for this model are given in table form and a cubic spline interpolation was used to obtain their values as functions of the radius.

The numerical integration of model P is performed as follows:

- a. a homogeneous earth model is used to obtain nominal values for the radial functions ($y_1, y_2, y_3, y_4, y_5, y_6$) at a point within the inner solid core, i. e., $r_0 = 6.371 \times 10^6$ cm. The system of differential Equations (6.3) is numerically integrated outwards to the boundary between the solid inner core and the liquid core. Since y_2 vanishes in the liquid core, Equations (6.7) yield:

$$\begin{aligned} \{y_2\} &= -y_2 \\ \{y_1\} &= (1/\rho_0 g_0) \{y_2\} \\ \{y_6\} &= -4\pi G \rho_0 \{y_1\} \\ \{y_5\} &= 0 \end{aligned} \tag{10.1}$$

The third Equation (6.6) yields the value of y_3 within the liquid core.

There remains the condition matching the values of y_4 at the boundary,

i. e.,

$$\text{SC} \{y_4\}_{\text{LC}} = 0 \quad (10.2)$$

Equation (6.6) are then integrated outwards throughout the liquid core to the mantle boundary.

- b. the homogeneous earth model yields nominal values for the variables (y_1, y_3, y_5) at the surface of the earth where y_2 and y_4 are required to vanish. The value of y_6 is obtained from Equations (6.8) and (6.9), Equations (6.3) are then integrated inwards to the liquid core boundary.
- c. the two sets of solutions meeting at the liquid core-mantle boundary must satisfy the conditions given by Equations (6.7), i.e.,

$$\begin{aligned} \text{LC} \{y_2\}_{\text{M}} - \rho_0 g_0 \text{LC} \{y_1\}_{\text{M}} &= 0 \\ \text{LC} \{y_4\}_{\text{M}} &= 0 \\ \text{LC} \{y_5\}_{\text{M}} &= 0 \\ \text{LC} \{y_6\}_{\text{M}} - 4\pi G \rho_0 \text{LC} \{y_1\}_{\text{M}} &= 0 \end{aligned} \quad (10.3)$$

- d. a general purpose adaptive iterator for nonlinear problems (Campbell et al.) is used in order to satisfy the five conditions expressed by Equations (10.2) and (10.3), which play the role of dependent variables. The independent variables subject to variation are the values of $(y_1, y_2, y_3, y_4, y_5, y_6)$ at $r_0 = 6.371 \times 10^6$ cm and the values of (y_1, y_3, y_5) at the surface of the earth. The numerical integration package consists of an Adams-Moulton, Runge-Kutta fourth order.

The numerical integration of model M_3 follows a similar procedure but there are some differences which are outlined below:

- a. the absence of a solid inner core in this model requires that nominal values of (y_5, y_6) obtained from the homogeneous solution at $r_0 = 6.371 \times 10^6$ cm be used in the integration of Equations (6.6) throughout the liquid core.
- b. the value of the gravitational force, g_0 , is obtained from the integration of an additional differential equation (Pekeris and Jarosch, 1958) i. e.,

$$\frac{dg_0}{dr} + \frac{2}{r} g_0 = 4\pi G\rho_0 \quad (10.4)$$

Nominal initial values of g_0 for the integration of Equation (10.4) are obtained from the homogeneous solution at $r_0 = 6.371 \times 10^6$ cm and at the surface of the earth. Model P does not require this procedure since the density is given by polynomials.

- c. the adaptive iterator uses the values of (y_5, y_6, g_0) at r_0 and the values of (y_1, y_3, y_5, g_0) at the surface of the earth as independent variables in order to satisfy the set of conditions expressed by Equations (10.3) and the condition on g_0 at the liquid core-mantle boundary, i. e.,

$${}_{LC} \{g_0\}_M = 0 \quad (10.5)$$

Once the adaptive iterator has converged to a set of initial conditions the solution trajectories for the radial functions have been obtained. Figures 10.1-10.12

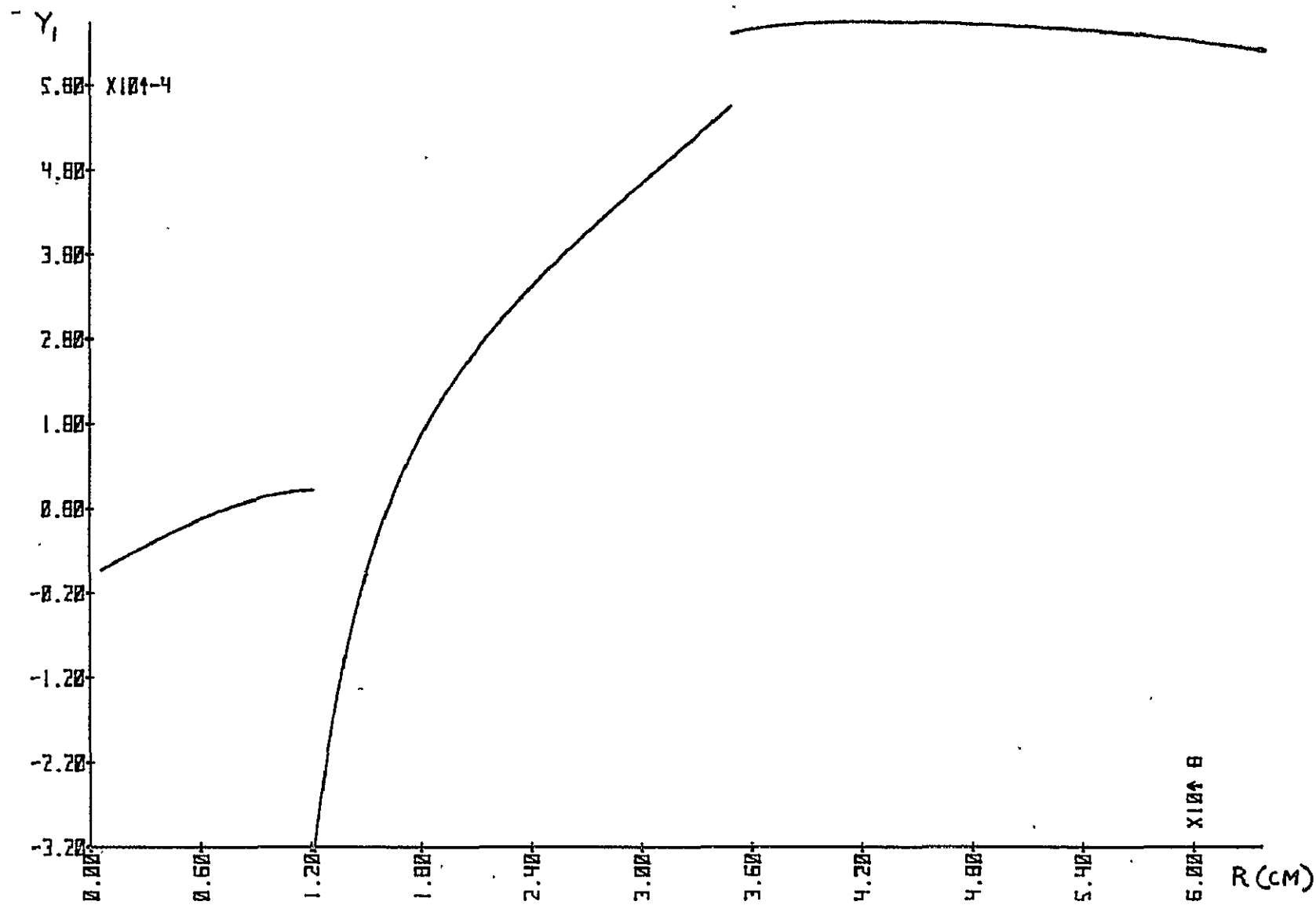


Figure 10.1. y_1 vs. r , Model P

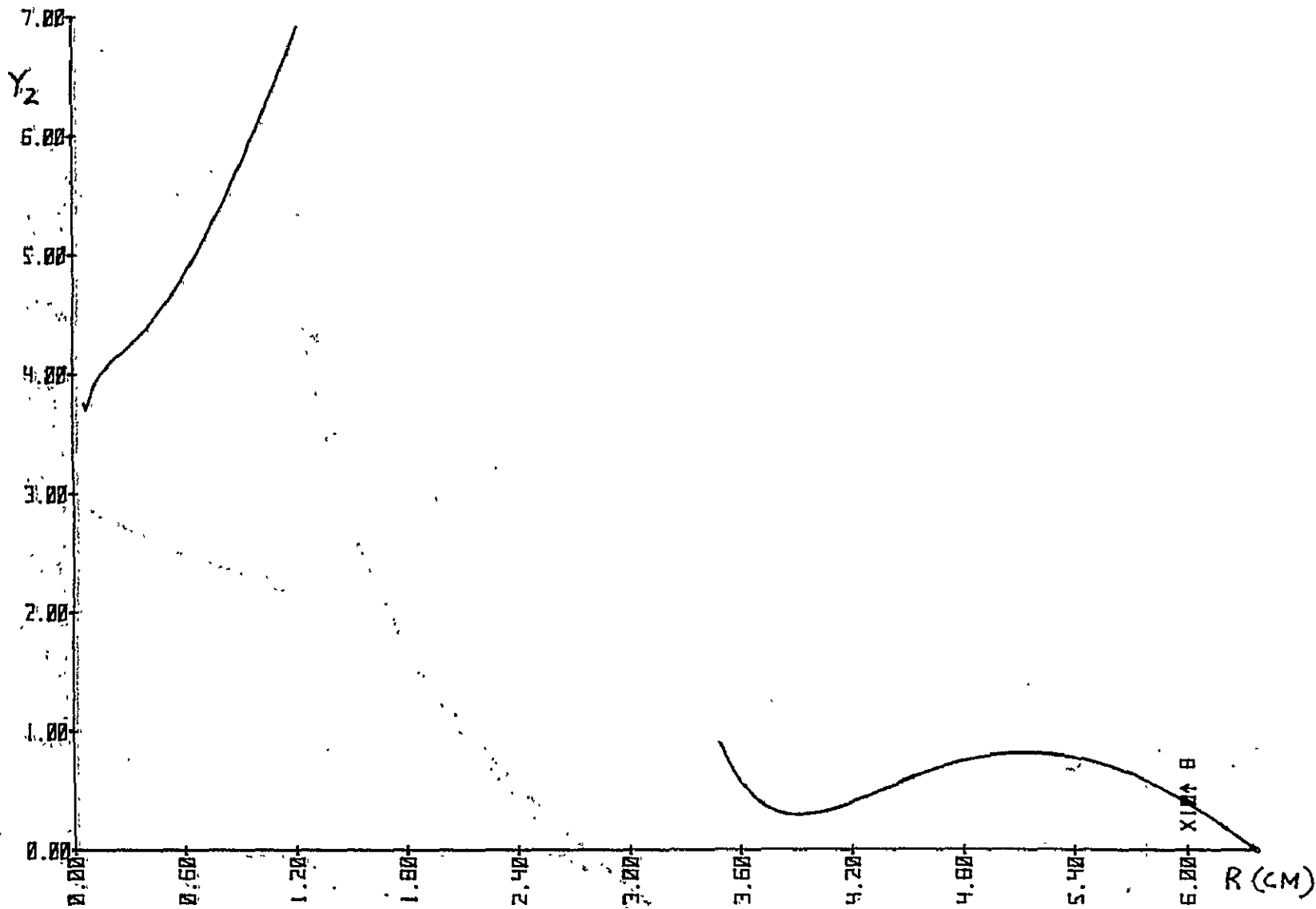


Figure 10.2. y_2 vs. r , Model P

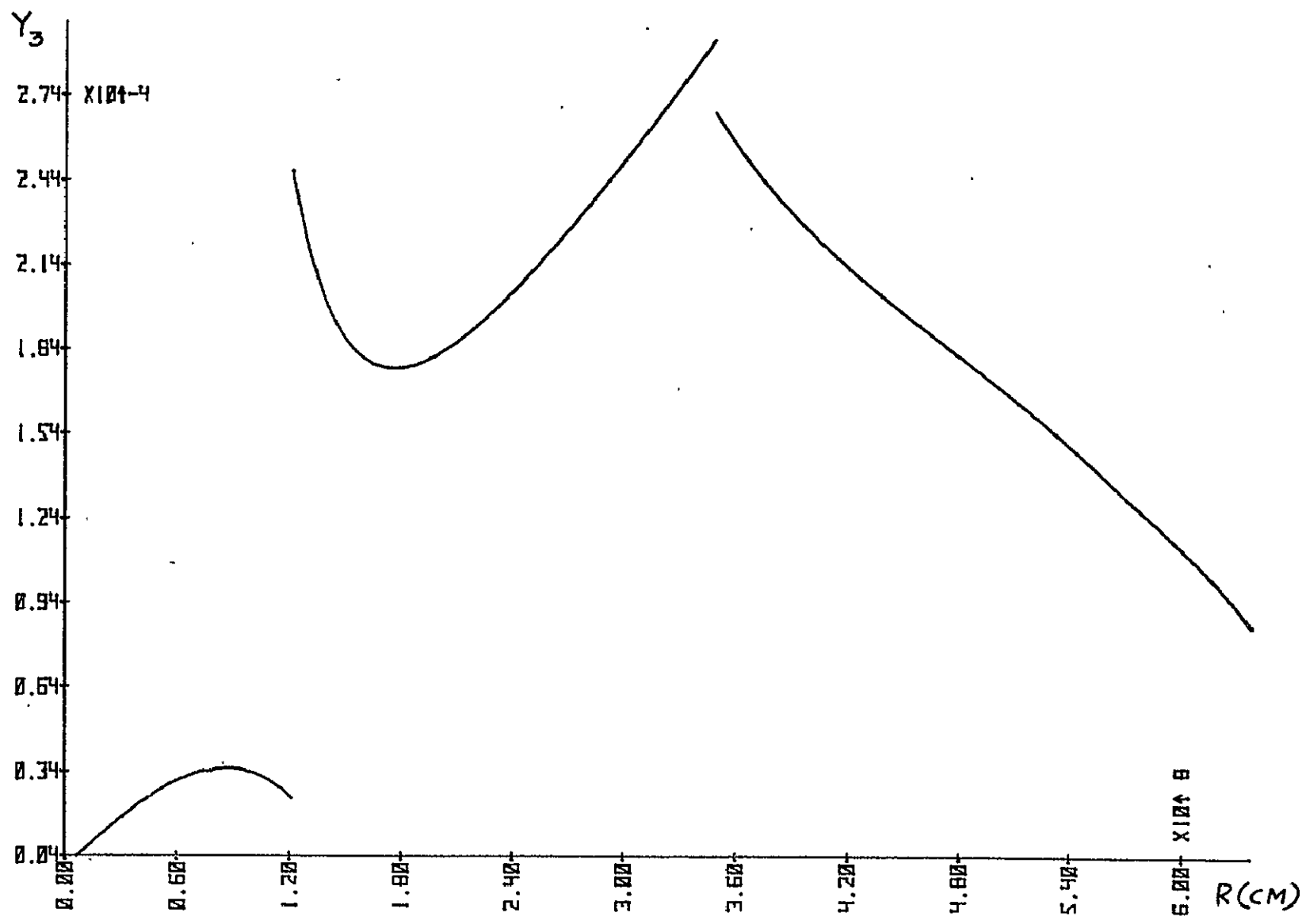
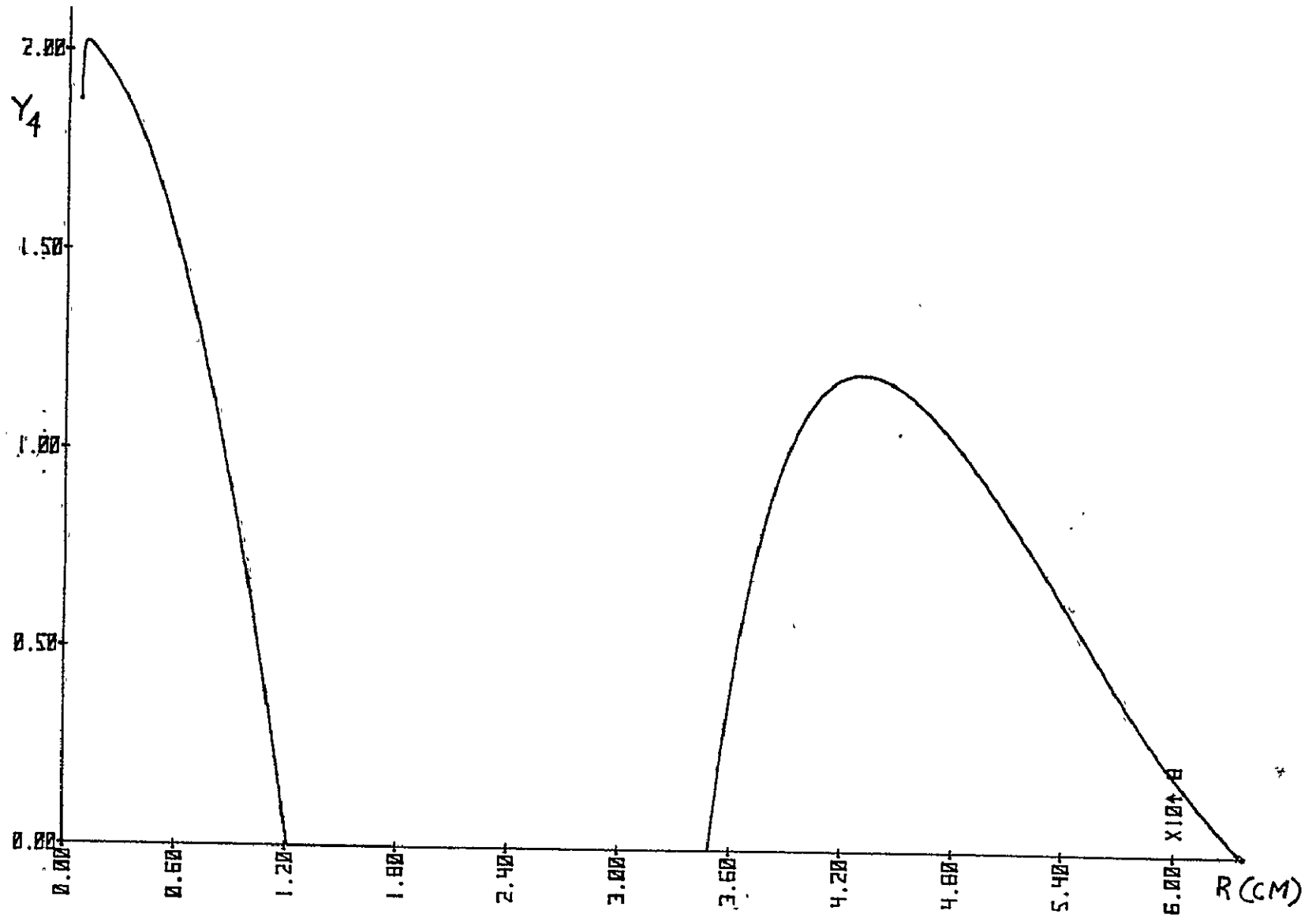


Figure 10.3. y_3 vs. r , Model P

Figure 10.4. y_4 vs. r , Model P

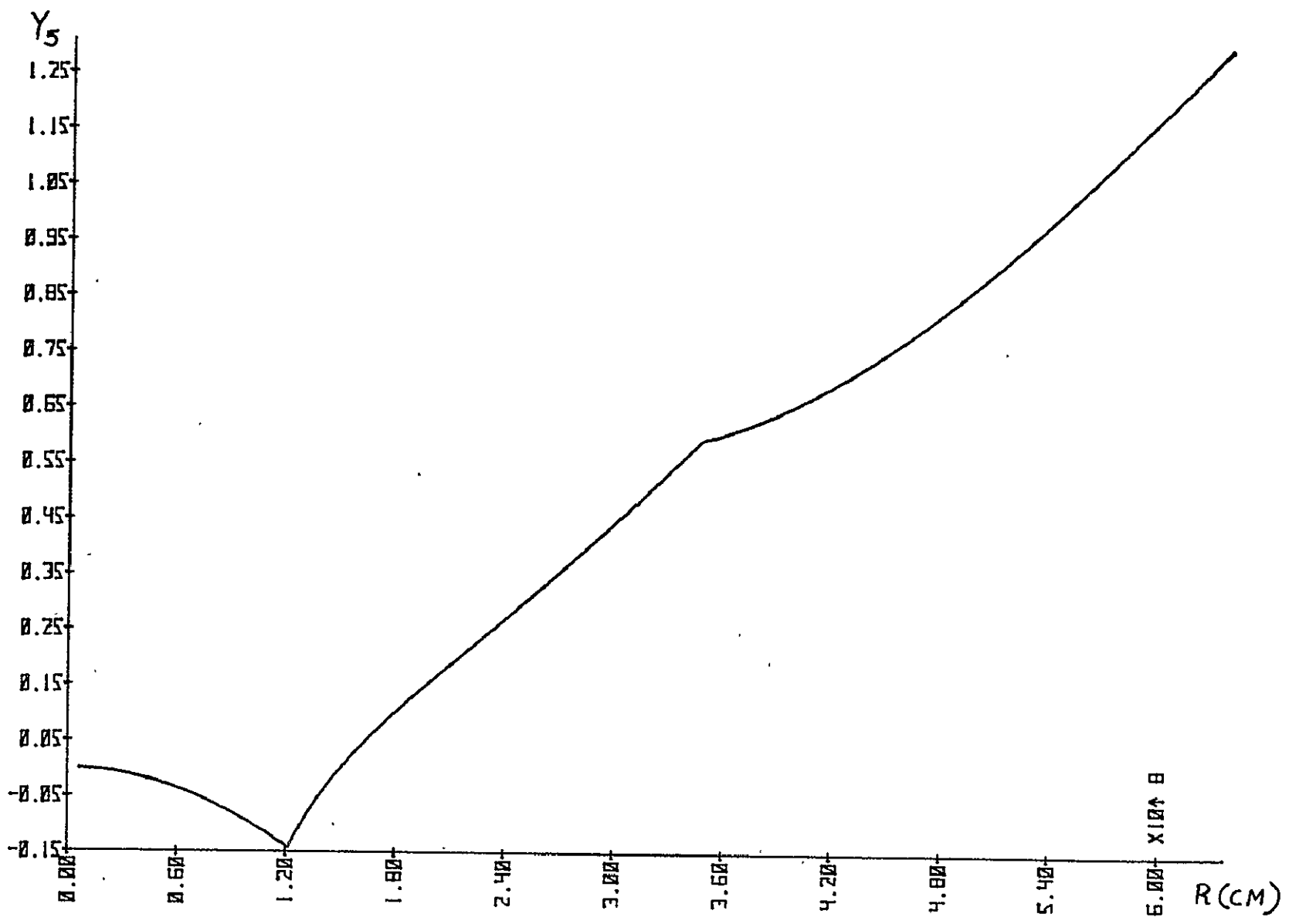


Figure 10.5. y_5 vs. r , Model P

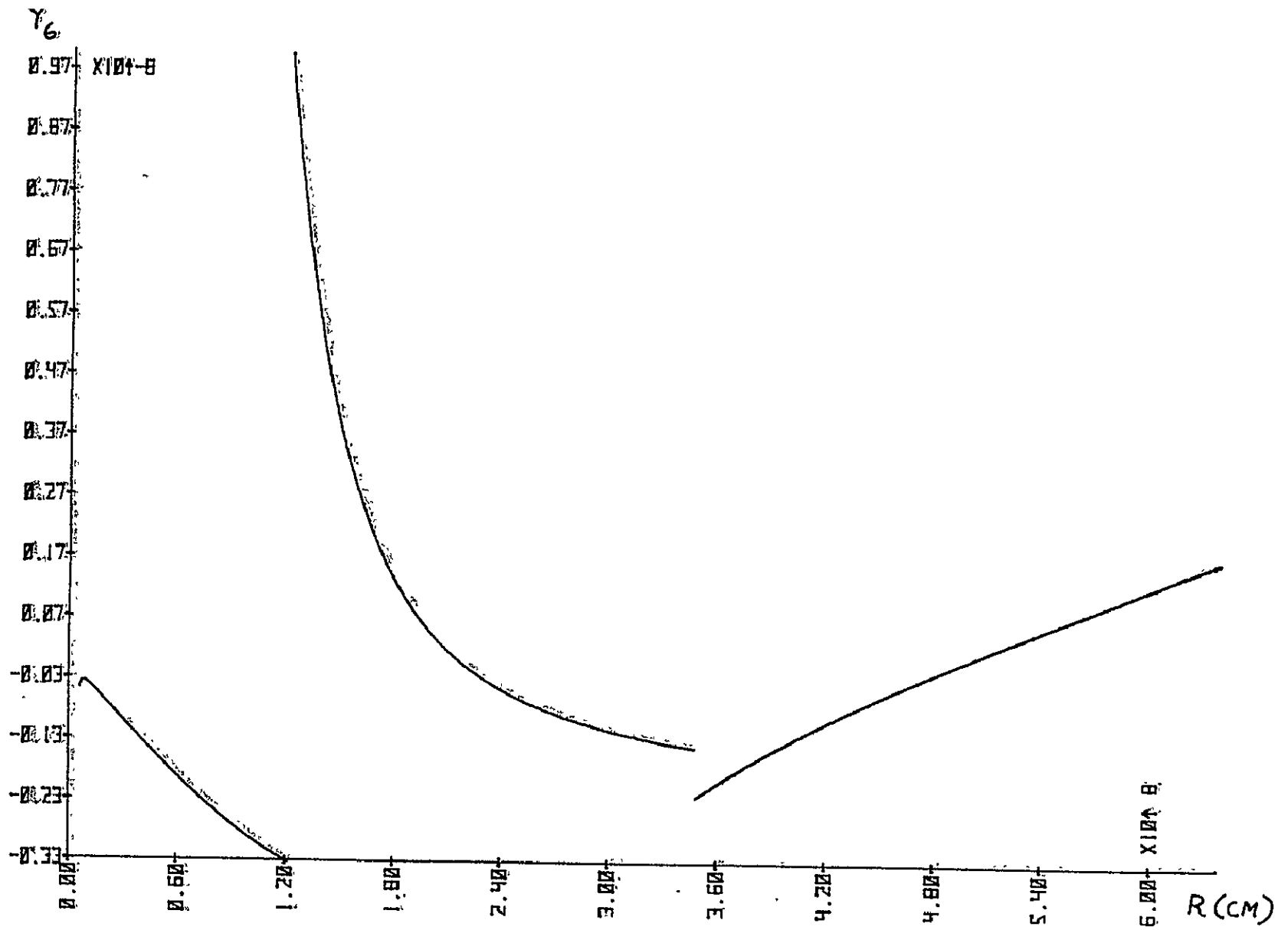


Figure 10.6. y_6 vs. r . Model P

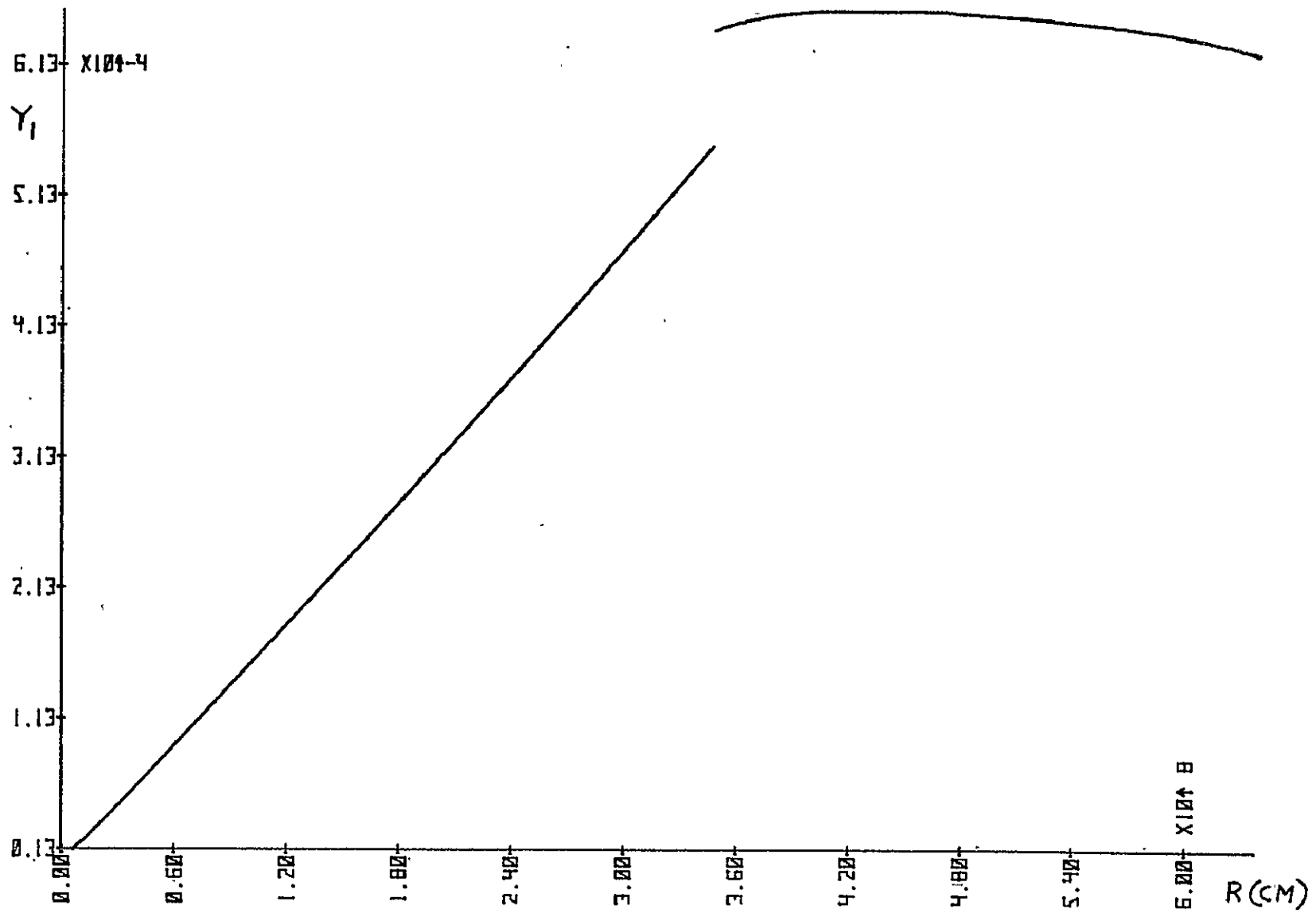


Figure 10.7. y_1 vs. r , Model M_3

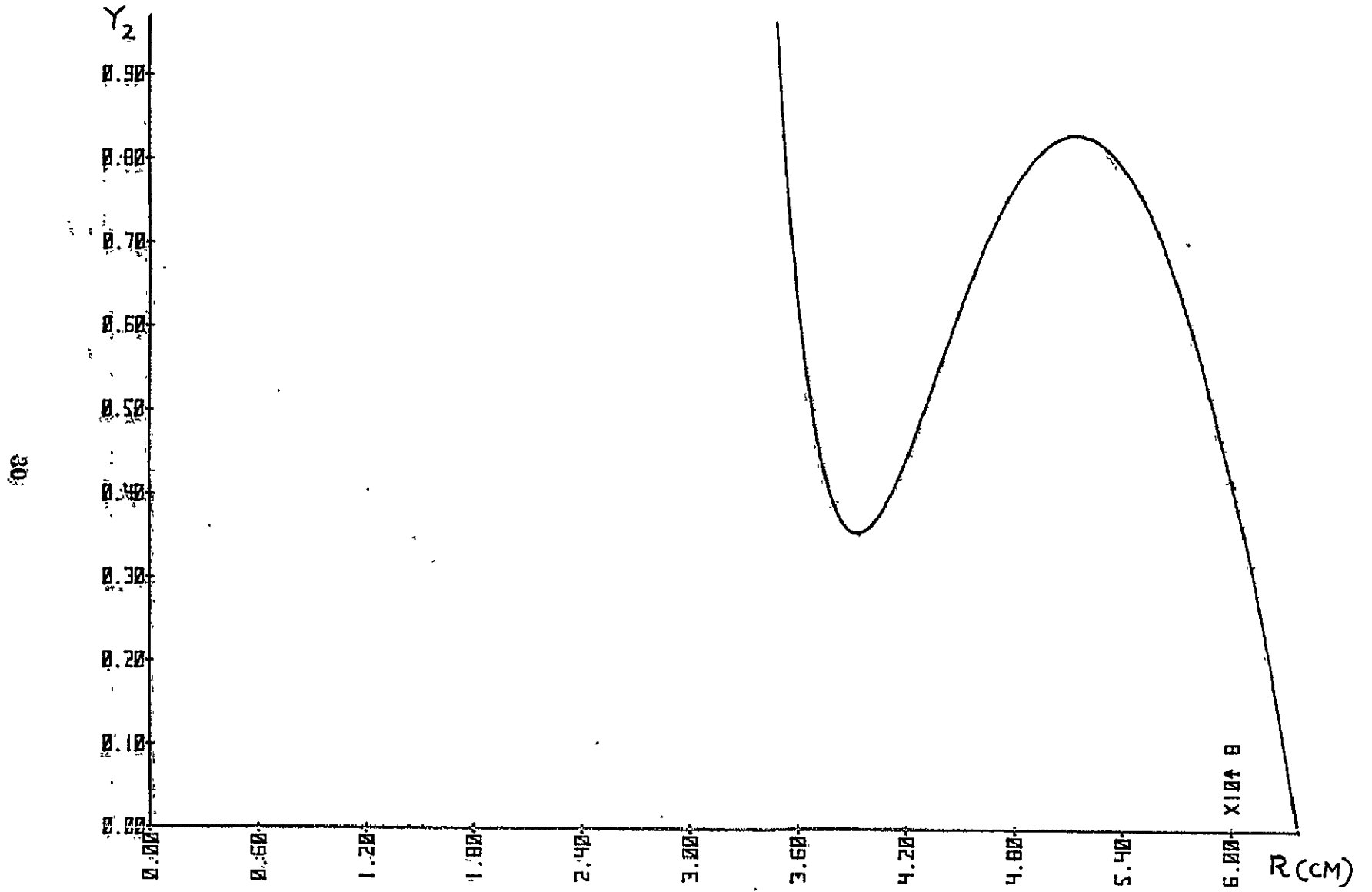


Figure 10.8. y_2 vs. r , Model M_3

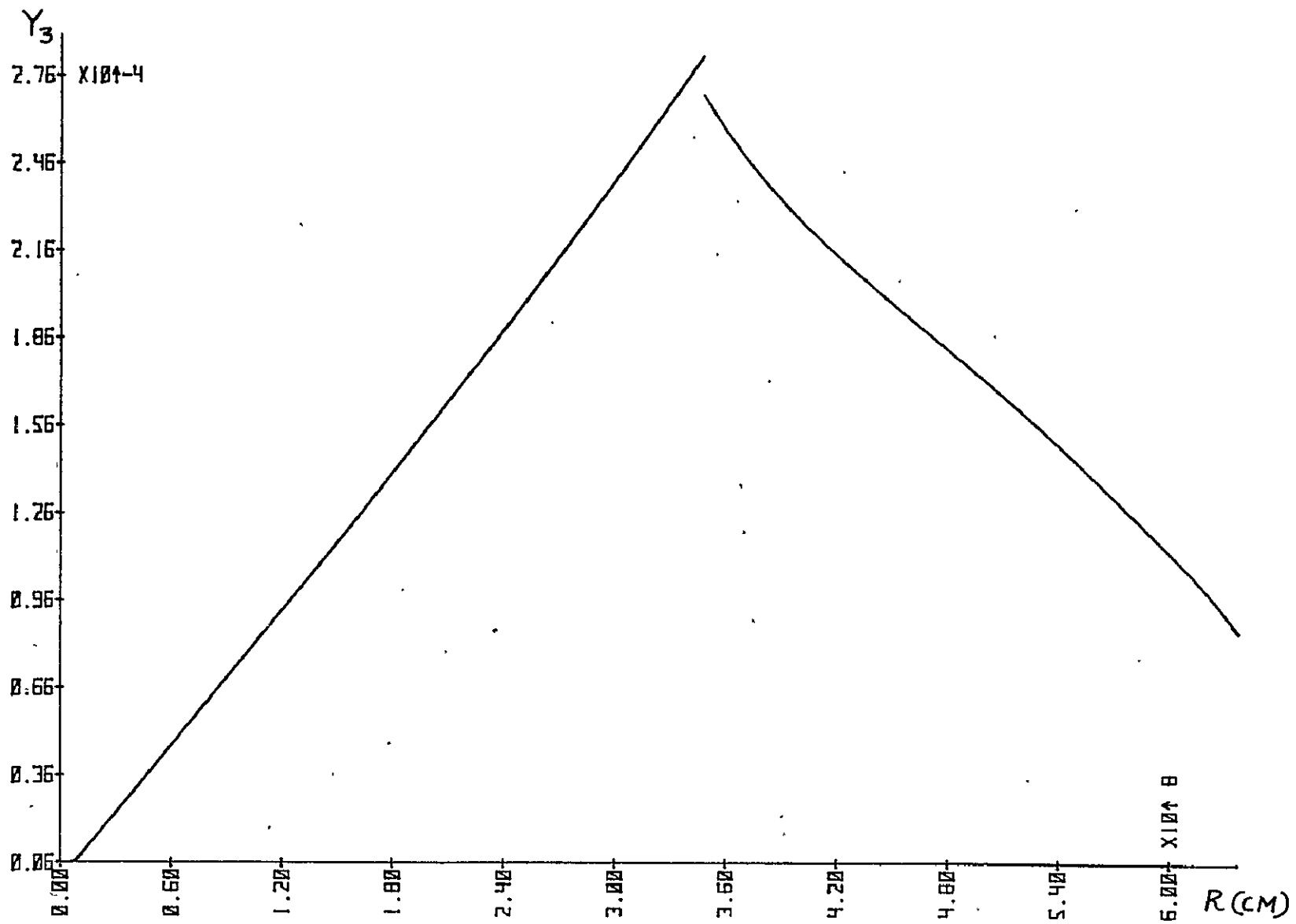


Figure 10.9. y_3 vs. r , Model M_3

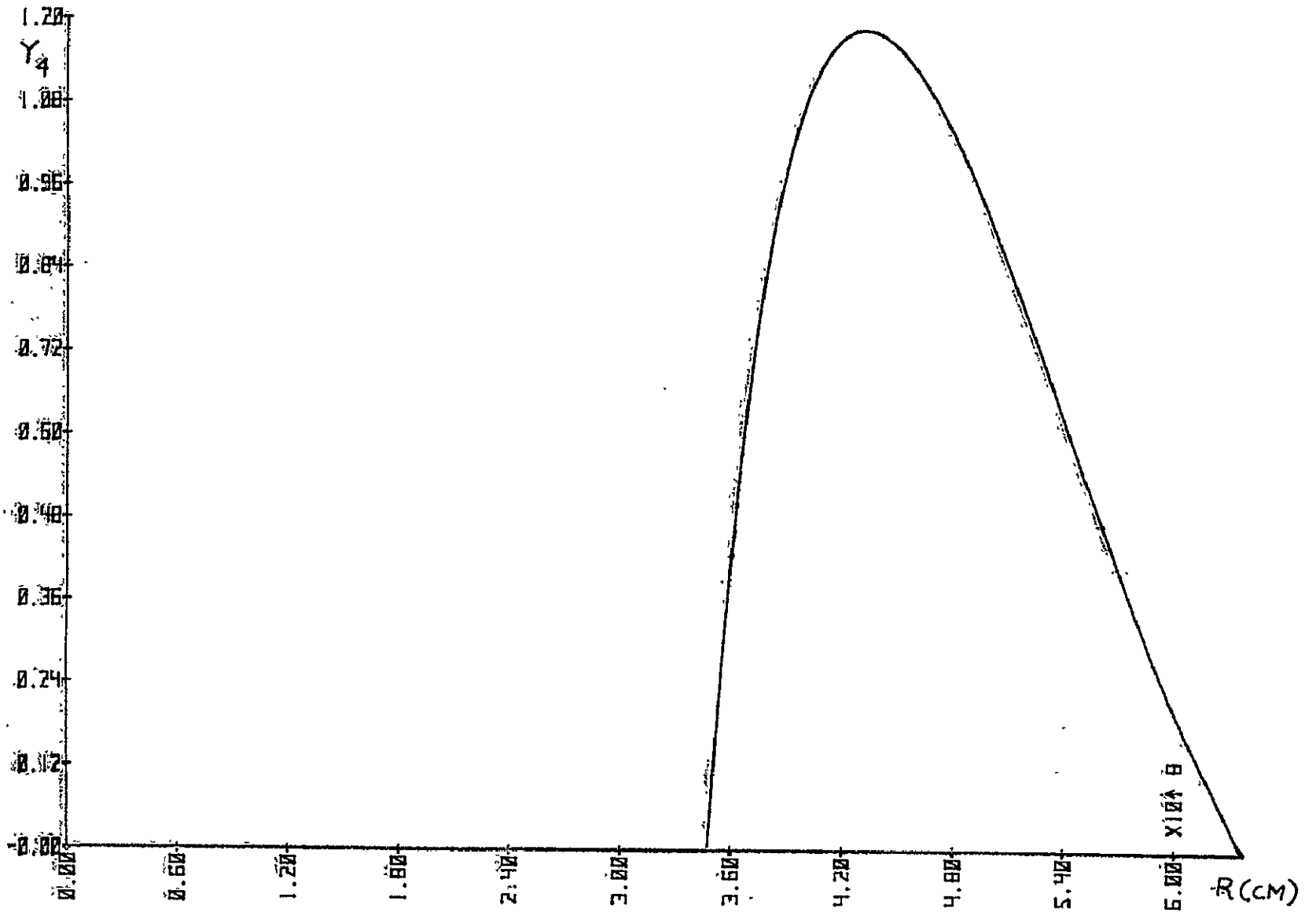


Figure 10.10. Y_4 vs. r . Model M.

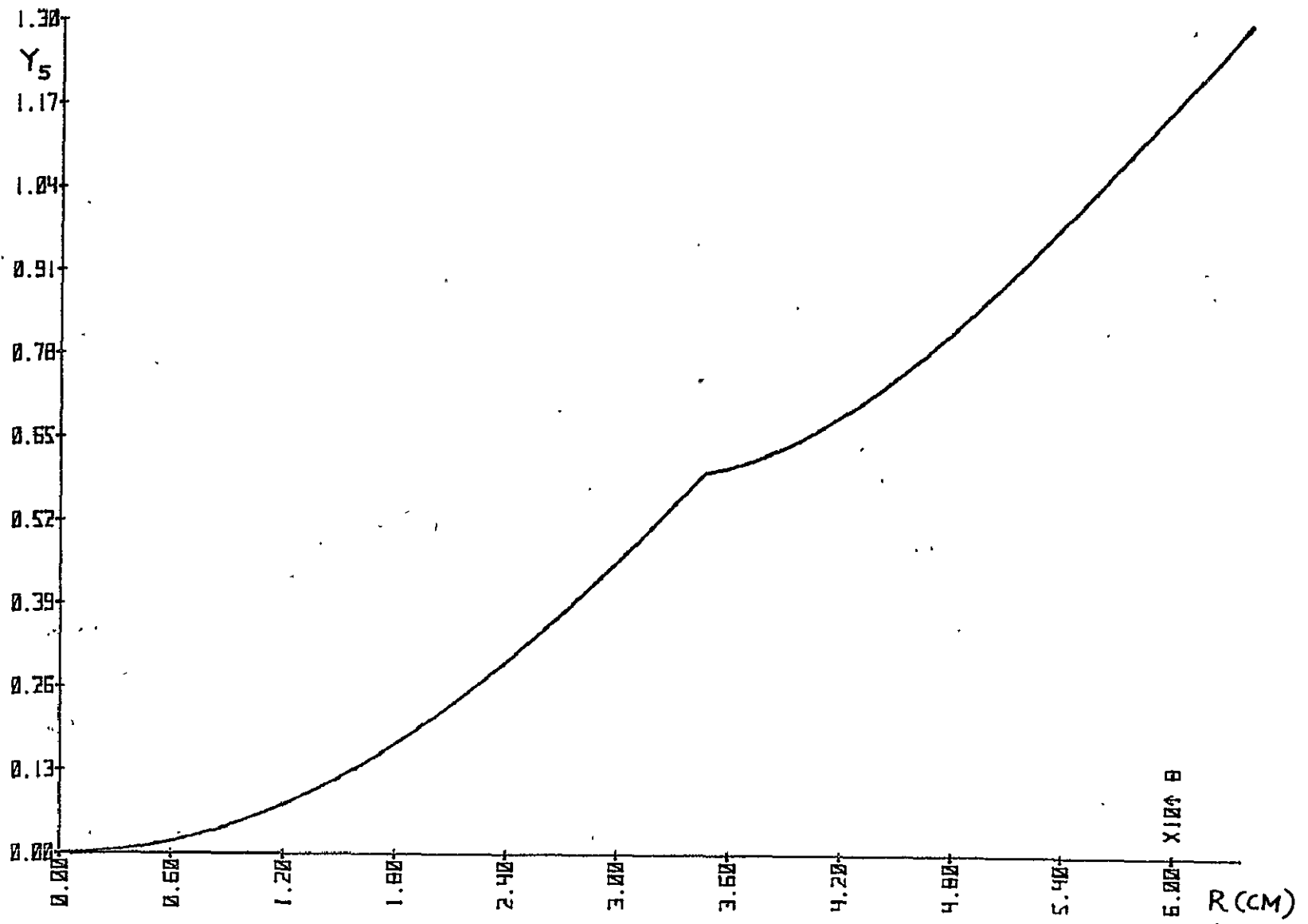


Figure 10.11. y_5 vs. r , Model M_3

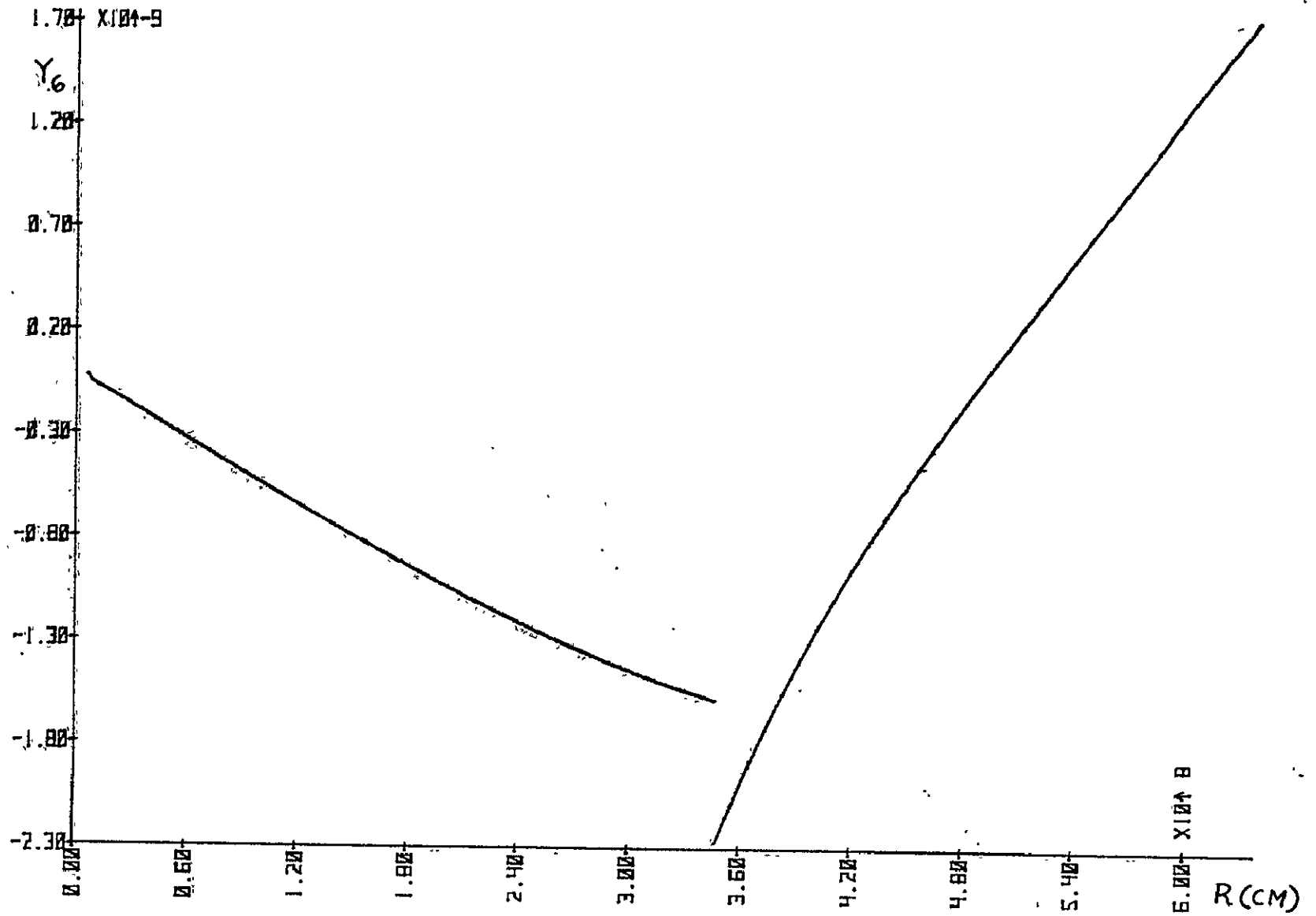


Figure 10.12. y_6 vs. r , Model M_3

below give the results for the P and M₃ models. The units for the radial functions are omitted in the figures, they are given by Equations (5.7), (5.8), (6.1) and (6.2).

11. NUMERICAL RESULTS AND CONCLUSIONS

The magnitude of the pole shift can be obtained from the following equation (Ben-Menahem and Israel, 1970):

$$MS = \frac{a\omega_E}{Af_0} (\Delta I_{xz}^2 + \Delta I_{yz}^2)^{1/2} \quad (11.1)$$

where a is the radius of the earth, ω_E the mean angular velocity of the diurnal rotation, f_0 is the angular frequency of the free Chandler wobble and A is the mean equatorial moment of inertia. The following values were used in the computation

$$a = 6.371 \times 10^8 \text{ cm}$$

$$\omega_E = 7.292 \times 10^{-5} \text{ rad/sec}$$

$$f_0 = 1.69 \times 10^{-7} \text{ rad/sec}$$

$$A = 8.016 \times 10^{44} \text{ gm cm}^2$$

The direction of the shift is given by

$$AS = \arctan \left(\frac{\Delta I_{yz}}{\Delta I_{xz}} \right) \quad (11.2)$$

The change in the length of the day is calculated by means of the following equation (Munk and MacDonald, 1975, page 98)

$$\Delta \text{LOD} = \frac{\Delta I_{zz}}{C} (\text{LOD}) \quad (11.3)$$

where LOD is the mean length of the day and C is the mean polar moment of inertia. The following values were used in the computation:

$$\text{LOD} = 86,400 \text{ sec}$$

$$C = 8.043 \times 10^{44} \text{ gm cm}^2$$

The changes in the second degree coefficients of the geopotential are given by well known relations which are reproduced below:

$$\begin{aligned} \Delta C_2^0 &= (Q/2)(\Delta I_{xx} + \Delta I_{yy} - 2\Delta I_{zz}) \\ \Delta C_2^1 &= Q(\Delta I_{xz}) \\ \Delta S_2^1 &= Q(\Delta I_{yz}) \\ \Delta C_2^2 &= (Q/4)(\Delta I_{yy} - \Delta I_{xx}) \\ \Delta S_2^2 &= (Q/2)(\Delta I_{xy}) \\ Q &= 1/a^2 \bar{M} \end{aligned} \quad (11.4)$$

where M is the mass of the Earth,

$$\bar{M} = 5.975 \times 10^{27} \text{ gm}$$

In order to generate numerical results a seismic event has to be chosen. The source parameters corresponding to the Alaskan earthquake on March 28, 1964 are used, as given by Israel et al., 1973. The parameters giving the position of the source are the following:

$$\theta = 28.9^\circ$$

$$\phi = 212.4^\circ$$

$$\alpha = 225^\circ$$

where θ denotes colatitude, ϕ the longitude and α the fault azimuth. The depth of the source is allowed to take the values of 20, 60, 100 and 200 km, and numerical results are given for each case. The magnitude of the source is determined by the slip magnitude Δu and the fault area Σ ,

$$\Delta u = 20 \text{ meters}$$

$$\Sigma = 70,000 \text{ km}^2$$

The source mechanism is specified by the dip angle δ and the slip angle λ . Numerical results are generated for the three assumptions below,

- i. vertical strike-slip: $\lambda = 0^\circ$, $\delta = 90^\circ$
- ii. vertical dip-slip: $\lambda = 90^\circ$, $\delta = 90^\circ$
- iii. dip-slip on 45° plane: $\lambda = 90^\circ$, $\delta = 45^\circ$

Tables 11.1-11.8 below give the results generated for the parametric earth model due to Dziewonski et al. denoted as model P, and the earth model M_3 of Landisman et al.

The results indicate that the magnitude of the pole displacement depends on the assumptions concerning the mechanism of the source, the same can be said

with respect to the direction of the shift and the change in the length of the day. The type of earth model used in the computations has some bearing in the results as is to be expected but not nearly as much as the type of source mechanism. The depth of the source introduces variations in the magnitude of the displacement and the change in the length of the day but the direction of shift is insensible to this parameter in the cases corresponding to a vertical strike-slip and a vertical dip-slip, in these cases the direction of shift is also invariable regardless of the type of earth model. Israel et al. (1973) used a different method to obtain the displacement of the pole for model M_3 , in general the results of this investigation are in agreement with those given by them.

REFERENCES

- Alterman, Z., H. Jarosch, and C. L. Pekeris, 1959, "Oscillations of the Earth", *Proceedings of the Royal Society, A*, 252, pp. 80-95.
- Ben-Menahem, A. and M. Israel, 1970, "Effects of Major Seismic Events on the Rotation of the Earth", *Geophysical Journal of the Royal astronomical Society*, 19, pp. 367-393.
- Crossley, D. J., and D. Gubbins, 1975, "Static Deformation of the Earth's liquid Core", *Geophysical Research Letters*, 2, pp. 1-4.
- Campbell, J, W. E. Moore, and H. Wolf, 1964, "Minmax: A General Purpose Adaptive Iterator for Nonlinear Problems", *Analytical Mechanics Associates, Inc.*
- Dziewonski, A. M., A. L. Hales, and E. R. Lapwood, 1975, "Parametrically Simple Earth Models consistent with Geophysical Data", *Physics of the Earth and Planetary Interiors*, 10, pp. 12-48.
- Israel, M., A. Ben-Menahem, and S. J. Singh, 1973, "Residual Deformation of Real Earth Models with Application to the Chandler Wobble", *Geophysical Journal of the Royal astronomical Society*, 32, pp. 219-247.

Landisman, M., Y. Sato, and T. Nafe, 1965, "Free vibrations of the Earth and the properties of its deep interior", *Geophysical Journal of the Royal astronomical Society*, 9, pp. 439-502.

Love, A. E. H., 1927, A Treatise on the Mathematical Theory of Elasticity, Cambridge University Press, Dover Publications, 1944.

Munk, W. H., and G. J. F. MacDonald, 1975, The Rotation of the Earth, Cambridge University Press.

Pekeris, C. L., and H. Jarosch, 1958, "The Free Oscillations of the Earth", in Contributions in Geophysics, Vol. I, Pergamon Press, London, England.

Rice, J. R., and M. A. Chinnery, 1972, "On the Calculation of Changes in the Earth's Inertia Tensor due to Faulting", *Geophysical Journal of the Royal astronomical Society*, 29, pp. 79-90.

Smylie, D. E., and L. Mansinha, 1971, "The Elasticity Theory of Dislocations in Real Earth Models and Changes in the Rotation of the Earth", *Geophysical Journal of the Royal astronomical Society*, 23, pp. 329-354.

Sanchez, B. V., 1974, "Rotational Dynamics of Mathematical Models of the Nonrigid Earth", A. M. R. L. 1066, The University of Texas at Austin.

Takeuchi, H., M. Saito, and N. Kobayashi, 1962, "Statical Deformations and Free Oscillations of a Model Earth", Journal of Geophysical Research, 67, pp. 1141-1154.

Table 11.1
Pole Shift (cm)

		20 km	60 km	100 km	200 km
Vertical	P	7.3	17.4	18.3	18.4
Strike-Slip	M ₃	8.1	17.3	16.6	17.8
Vertical	P	2.0	7.3	13.1	27.7
Dip-Slip	M ₃	2.1	7.7	13.8	28.9
Dip-Slip on 45° Plane	P	19.4	45.3	46.2	45.4
	M ₃	22.6	46.7	43.7	44.3

Table 11.2
Angle (Degrees)

		20 km	60 km	100 km	200 km
Vertical	P	-147.6	-147.6	-147.6	-147.6
Strike-Slip	M ₃	-147.6	-147.6	-147.6	-147.6
Vertical	P	91.0	91.0	91.0	91.0
Dip-Slip	M ₃	91.0	91.0	91.0	91.0
Dip-Slip on 45° Plane	P	-35.6	-38.0	-43.2	-52.2
	M ₃	-28.4	-33.0	-35.7	-47.1

Table 11.3
 $\Delta \text{LOD (sec)} \times 10^8$

		20 km	60 km	100 km	200 km
Vertical	P	127	302	317	319
Strike-Slip	M ₃	140	300	287	308
Vertical	P	-52	-189	-339	-718
Dip-Slip	M ₃	-56	-199	-357	-748
Dip-Slip on 45° Plane	P	741	1686	1627	1404
	M ₃	910	1815	1662	1482

Table 11.4
 $\Delta C_{20} \times 10^{10}$

		20 km	60 km	100 km	200 km
Vertical	P	-0.073	-0.174	-0.182	-0.184
Strike-Slip	M ₃	-0.080	-0.172	-0.165	-0.177
Vertical	P	0.030	0.109	0.195	0.413
Dip-Slip	M ₃	0.032	0.114	0.205	0.430
Dip-Slip on 45° Plane	P	-0.426	-0.971	-0.937	-0.808
	M ₃	-0.524	-1.045	-0.957	-0.853

Table 11.5

 $\Delta C_{21} \times 10^{10}$

		20 km	60 km	100 km	200 km
Vertical	P	-0.075	-0.177	-0.186	-0.187
Strike-Slip	M ₃	-0.082	-0.176	-0.168	-0.180
Vertical	P	-0.0004	-0.001	-0.002	-0.006
Dip-Slip	M ₃	-0.0004	-0.001	-0.003	-0.006
Dip-Slip on 45° Plane	P	0.190	0.429	0.405	0.334
	M ₃	0.239	0.470	0.427	0.362

Table 11.6

 $\Delta S_{21} \times 10^{10}$

		20 km	60 km	100 km	200 km
Vertical	P	-0.047	-0.112	-0.118	-0.119
Strike-Slip	M ₃	-0.052	-0.111	-0.107	-0.114
Vertical	P	0.024	0.088	0.157	0.333
Dip-Slip	M ₃	0.026	0.092	0.166	0.347
Dip-Slip on 45° Plane	P	-0.136	-0.336	-0.380	-0.431
	M ₃	-0.129	-0.306	-0.307	-0.390

Table 11.7

 $\Delta C_{22} \times 10^{11}$

		20 km	60 km	100 km	200 km
Vertical	P	-0.394	-0.933	-0.979	-0.987
Strike-Slip	M ₃	-0.432	-0.928	-0.888	-0.952
Vertical	P	0.030	0.110	0.198	0.418
Dip-Slip	M ₃	0.033	0.116	0.208	0.436
Dip-Slip on 45° Plane	P	0.283	0.685	0.750	0.808
	M ₃	0.289	0.650	0.639	0.751

Table 11.8

 $\Delta S_{22} \times 10^{11}$

		20 km	60 km	100 km	200 km
Vertical	P	-0.839	-1.984	-2.081	-2.099
Strike-Slip	M ₃	-0.919	-1.972	-1.887	-2.024
Vertical	P	-0.070	-0.253	-0.453	-0.958
Dip-Slip	M ₃	-0.075	-0.265	-0.477	-0.998
Dip-Slip on 45° Plane	P	0.603	1.457	1.595	1.719
	M ₃	0.614	1.383	1.358	1.597

FIGURE CAPTIONS

Figure 10.1. y_1 vs. r , Model P

Figure 10.2. y_2 vs. r , Model P

Figure 10.3. y_3 vs. r , Model P

Figure 10.4. y_4 vs. r , Model P

Figure 10.5. y_5 vs. r , Model P

Figure 10.6. y_6 vs. r , Model P

Figure 10.7. y_1 vs. r , Model M_3

Figure 10.8. y_2 vs. r , Model M_3

Figure 10.9. y_3 vs. r , Model M_3

Figure 10.10. y_4 vs. r , Model M_3

Figure 10.11. y_5 vs. r , Model M_3

Figure 10.12. y_6 vs. r , Model M_3